



Effect of soft Bi particles on grain refinement during severe plastic deformation

Hai-long JIA, K. MARTHINSEN, Yan-jun LI

Department of Materials Science and Engineering,
Norwegian University of Science and Technology, Trondheim 7491, Norway

Received 1 May 2016; accepted 18 October 2016

Abstract: Two aluminum alloys, Al–8Zn and Al–6Bi–8Zn were subjected to equal channel angular pressing (ECAP) up to 5 passes at room temperature. The microstructural evolution and the grain refinement behavior of these alloys were systematically studied by electron backscatter diffraction (EBSD). After 5 passes of ECAP, ultrafine grained microstructures formed in both alloys. However, the grain structure in the Al–6Bi–8Zn alloy is much finer than that of Al–8Zn alloy, showing that the soft Bi particles have a strong influence on enhancing the grain refinement during ECAP. The strengths of the ECAP-processed materials were measured by hardness test and it showed that after 5 passes of ECAP, the hardness of the Al–6Bi–8Zn alloy was higher than that of the Al–8Zn alloy. The effects of soft Bi particles on the deformation behavior during ECAP and the final strength of the Al–6Bi–8Zn alloy were discussed.

Key words: Al alloys; equal channel angular pressing (ECAP); Bi particle; grain refinement; hardness

1 Introduction

Alloys with a miscibility gap in the liquid state, such as Al–Bi, Al–Pb and Al–In, are potential materials for the application in advanced bearings in automotive industry [1]. The so-called hypermonotectic alloys with gross compositions above the monotectic one would be especially useful because the volume fraction of the soft inclusions is sufficiently high to produce bearings with a drastically low friction coefficient and a very small wear resistance. Hypermonotectic Al–Bi (i.e. >3.4% Bi) alloys containing homogeneously distributed soft secondary phase Bi particles (melting temperature 271.3 °C) within an Al-enriched hardenable matrix can resist high pulsating loads and show good tribological properties. Recently, European Union has proscribed the use of Pb-containing alloys [2], so, hypermonotectic alloys have gained increased interest again. Therefore, developments of new Pb-free bearing materials are of great importance and alloys based on Al–Bi system are supposed to be good candidates to replace Al–Pb alloys. At the same time, another special advantage of the aluminum-based bearing materials is mass saving. So far, most of the research works have been conducted to understand the solidification behavior of Al–Bi alloys

and improve the distribution of Bi particles by different methods [3–5]. For example, SILVA et al [6,7] studied microstructural development as well as thermal parameters during transient directional solidification of Al–Bi alloys.

Equal channel angular pressing (ECAP) has been used to produce ultrafine grained (UFG) materials at a relatively low cost for many years [8]. However, studies of alloy composites containing soft easily deformable secondary phase particles distributed in a ductile hardenable matrix processed by ECAP are few [9]. Recently, ZHA et al [9] investigated the deformation behavior of Al–8Bi alloy using ECAP and found that the soft Bi particles contribute to matrix grain refinement. But the strength of the binary Al–Bi alloy is too low, so the aim of the present study is to improve the strength of Al–Bi alloy (by adding Zn into the Al–Bi alloy). The influence of soft secondary phase particles on grain refinement in hypermonotectic Al alloys containing Bi during ECAP process was investigated. At the same time, the corresponding hardness was briefly reported.

2 Experimental

The materials used in the present work were Al–8%Zn and Al–6%Bi–8%Zn ingots which were

produced by melting 99.999% purity Al, Zn and Bi in a clay-graphite crucible and cast in an insulated and bottom-chilled Cu mould. It is noted that 0.5%Al–Ti–B grain refiner was added into the melt to get fine grains. Bars with dimensions of 100 mm × 19.5 mm × 19.5 mm were machined from ingots for the ECAP process. Before ECAP, to lower the friction during pressing, samples were coated with a thin layer of a graphite lubricant. Then, these bars were processed by ECAP through a 90° die via route Bc (samples was rotated by 90° in the same sense between each pass) at room temperature, which leads to an imposed equivalent strain of about 1.0 per pass [8].

Samples from the uniformly deformed central region of the ECAP-processed billets were chosen for microstructure observation and hardness test. The deformed structure was characterized on the longitudinal section by electron backscatter diffraction (EBSD). The samples were ground mechanically on abrasive papers containing SiC particles to a level of 4000 grit and finally polished with the 1 μm diamond paste. It is noted that prior to the EBSD examination, the sample surfaces were ion milled by using the Hitachi IM 3000 machine at a high tilt angle of ~70° and a gas flow rate of ~0.08 mL/min for 45 min at 3.5 V. EBSD was performed using a Hitachi SU–6600 field emission gun SEM (FEG-SEM) equipped with a Nordif EBSD detector and TSL-OIM software. The Vickers hardness measurements were performed using a DKV–1S Vickers hardness testing machine under a load of 1 kg with a loading time of 15 s. The hardness values obtained were averaged from at least 10 separate measurements to minimize the scatter. The equivalent circular diameter of the Bi particles was measured using the Image J software. Four BSE images for each sample were used for image analysis.

3 Results and discussion

3.1 Microstructural characterization

3.1.1 As-cast microstructure

As shown in Fig. 1(a), the microstructure of the as-cast Al–8Zn alloy consisted of α (Al) grains with an average size of ~50 μm which was almost the same as the grain size of the matrix of Al–6Bi–8Zn alloy. In Fig. 1(b), the black spheres were Bi particles. Some of the Bi particles were along the grain boundaries and some are inside of the grains of the matrix. The average size of the Bi particles was measured to be approximately 5 μm by using the Image J software.

3.1.2 Deformation structure after room temperature ECAP

EBSD analysis was conducted on the longitudinal section of the 1 pass and 5 passes samples and the

corresponding maps of the deformation microstructure developed after ECAP are shown in Fig. 2. The black areas are Bi particles in Figs. 2(b) and (d).

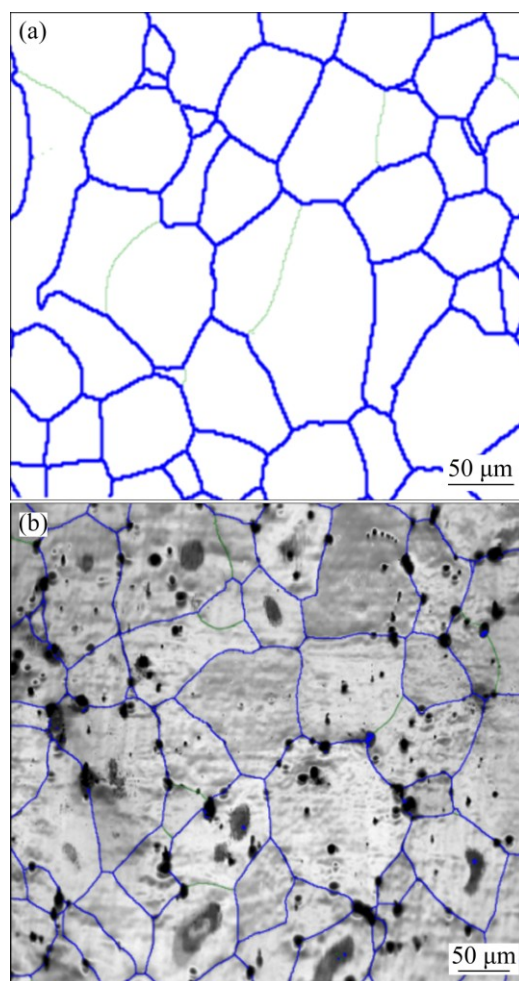


Fig. 1 Grain boundary map (EBSD) for as-cast Al–8Zn alloy (a) and image quality map (EBSD) for as-cast Al–6Bi–8Zn alloy (b) (Green and blue lines depict differences between neighbouring grid points $2^\circ < \theta < 15^\circ$ and $15^\circ < \theta < 180^\circ$, respectively)

After 1 pass of ECAP, as can be seen from Figs. 2(a) and (b), the coarse equiaxed grains in the initial as-cast state of these two alloys were deformed into elongated grains (several hundred micrometers long) bounded by high angle grain boundaries (HAGBs), mainly aligned at an angle of ~30° to the extrusion direction (ED). It can be also seen that many low angle boundaries (LAGBs) and deformation bands were developed in the elongated grains. The formation of such deformation bands is energetically easier for a constrained grain to deform by splitting into regions, operating on fewer than the five independent slip systems required for homogeneous deformation and strain is distributed over the different bands so as to collectively maintain compatibility with its neighbors [10,11].

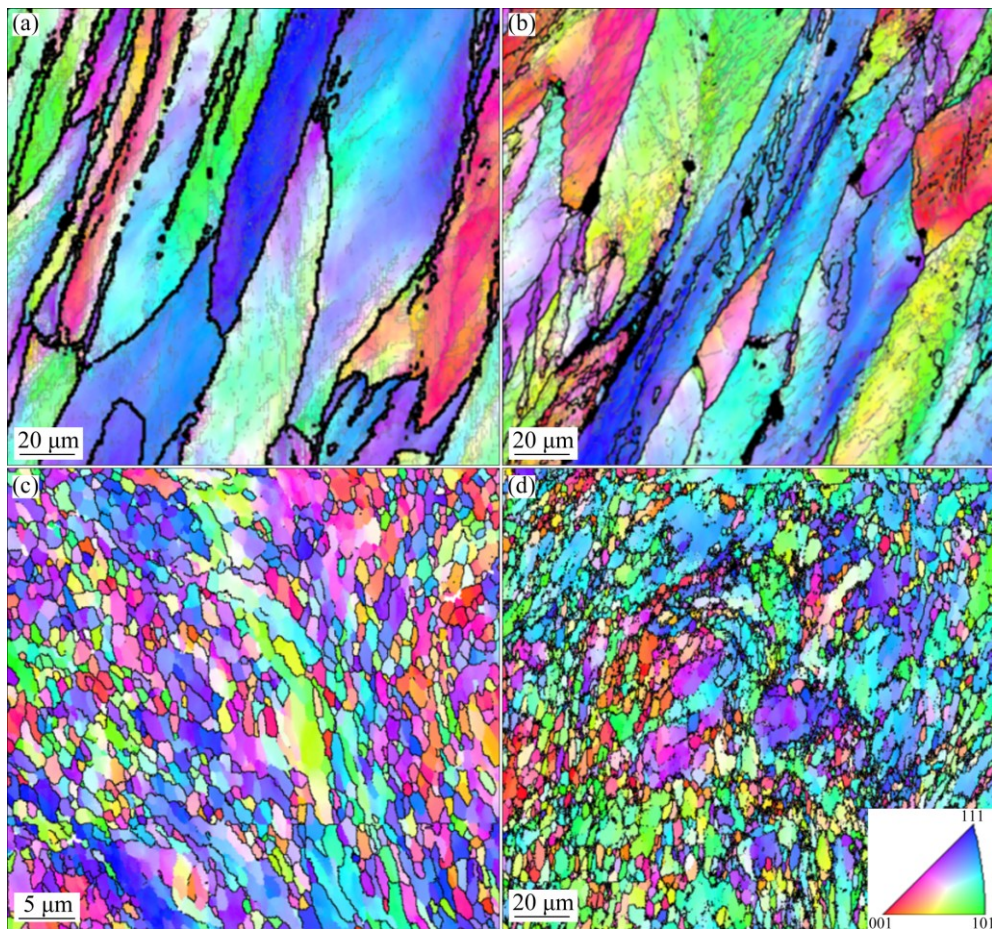


Fig. 2 EBSD images of ECAP-processed Al-8Zn alloy: (a) 1 pass and (c) 5 passes, Al-6Bi-8Zn alloy: (b) 1 pass and (d) 5 passes, where narrow grey and coarse black lines depict differences between neighbouring grid points $2^\circ < \theta < 15^\circ$ and $15^\circ < \theta < 180^\circ$ respectively, and insert in (d) is colour code for orientation maps

After 5 passes of ECAP, the coarse elongated grains were refined, resulting in an ultrafine equiaxed (sub)grain structure (Figs. 2(c) and (d)). However, it is obvious that there was no bimodal grain structure as that in Al-7Mg [12] processed by ECAP after 3 passes, which may be due to the low Zn content (mole fraction, %) and the solute strengthening capacity of Zn is much lower than that of Mg. The microstructure evolution during ECAP suggests that the grain refinement is mainly through the formation of subgrain and the progressive transformation of LAGBs into HAGBs in response to increasing strain. In Figs. 2(a) and (b), there were some HAGB segments formed inside of the elongated grains. The formation of discontinuous, short HAGB segments distributed heterogeneously among sub-boundaries of the original grains indicates that continuous dynamic recrystallization (CDRX) occurred during ECAP [13].

In order to find out the influence of soft Bi particles on the microstructural evolution of Al-6Bi-8Zn alloy, the measured (sub)grain size and HAGB fraction are shown in Fig. 3. From Fig. 3(a), we can see that the grain

size of the Al-8Zn alloy at a strain ε of ~ 5 (5 passes) was measured to be $\sim 1 \mu\text{m}$, which was significantly larger than that of the Al-6Bi-8Zn alloy. This implies that the presence of Bi particles significantly promoted grain refinement of the Al-6Bi-8Zn alloy containing Bi particles, resulting in the grain size of $\sim 0.5 \mu\text{m}$ at a strain of ~ 5 (5 passes). It is known that in severe plastic deformation (SPD) processing, a steady state grain size eventually reaches at ultra-high strains, which limits the achievable level of grain refinement [14,15]. This limit is controlled by the mobility of low and high angle grain boundaries. The introduction of secondary phase particles, which effectively pin grain boundaries, is a method for decreasing the limit grain size [16], allowing an increase in strength. As shown in Fig. 3(b), after 1 pass of ECAP, the misorientation angles for the Al-8Zn and Al-6Bi-8Zn alloy were still dominated by low angle grain boundaries. The fraction of HAGBs for the Al-6Bi-8Zn alloy was a little lower than that for the Al-8Zn alloy, which could be explained by the fact that at relatively low strains Bi particles contribute to the generation of LAGBs. However, an important feature

was the much larger fraction of HAGBs present in the Al–Bi–Zn alloy after 3 passes and 5 passes.

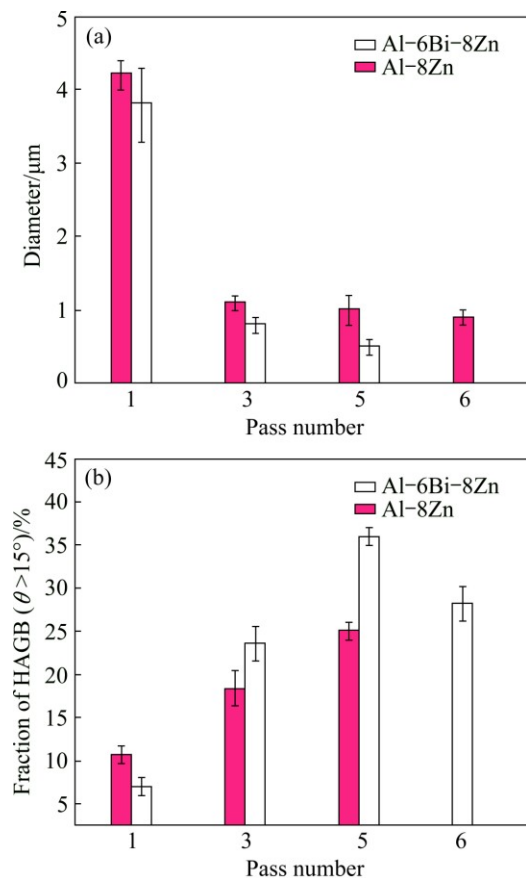


Fig. 3 (Sub)grain size development as function of increasing number of pass (a) and high angle grain boundary (HAGB) fraction development as function of increasing number of pass (b)

The generation of HAGBs as well as the development of new fine grains in the interior of original coarse grains of the Al–8Zn and Al–6Bi–8Zn alloys should be attributed to CDRX, which is an extended recovery process that proceeds by continuous absorption of dislocations at subgrain boundaries (LAGBs). During ECAP, LAGBs form in coarse grains, which evolve progressively into HAGBs with increasing strain due to accumulation of misorientations at LAGBs. However, the difference in the size and fraction of HAGBs in Al–8Zn and Al–6Bi–8Zn alloys should be ascribed to the presence of Bi particles. The role of the particles would therefore promote grain refinement (Figs. 2(c) and (d)).

In order to further study the influence of Bi particles on grain refinement during ECAP, high resolution EBSD maps (step size $0.05 \mu\text{m}$) were taken in regions around coarse Bi particles subjected to both low ($\epsilon=1$) and relative high ($\epsilon=5$) strain deformation (see Fig. 4). In these maps, the actual misorientation measurements of selected boundaries are indicated (in degree).

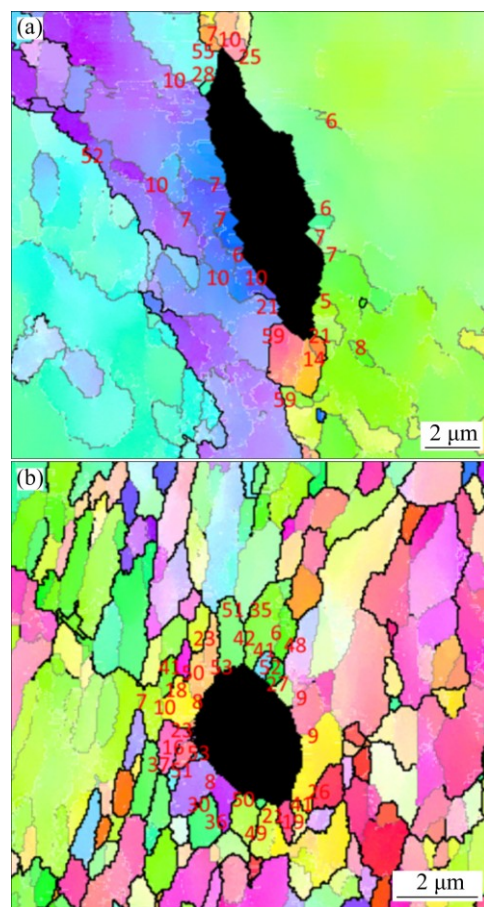


Fig. 4 High resolution ($0.05 \mu\text{m}$ step size) EBSD maps of Al–6Bi–8Zn alloy at different states: (a) 1 pass; (b) 5 passes (In the maps, orientation differences $\Delta\theta \geq 2^\circ$, $\Delta\theta \geq 5^\circ$ and $\Delta\theta \geq 15^\circ$ across boundaries are marked by thin white, thin gray and thick black lines, respectively)

After 1 pass of ECAP, large Bi particles inside of the original grains were elongated. Lots of boundaries emerged adjacent to the Bi particle (the unindexed black area in Fig. 4(a)). Moreover, a large number of equiaxed subgrains with misorientation $\sim 6^\circ$ – 10° formed around Bi particles. After 5 passes of ECAP, most of the subgrains evolved into grains and the amount of HAGBs with higher misorientation adjacent to the Bi particle were more than that in areas away from the particle. The present results therefore indicate that the soft Bi particles have stimulated the building up of the misorientation of grain boundaries and increased the density of HAGB grains with increasing strain. A piling up of misorientations around coarse hard $\text{Al}_{13}\text{Fe}_4$ particles similar to the present work were also observed by APPS et al [17] in a hard-particle-containing Al-alloy subjected to ECAP. Here, the soft Bi particles in the Al–6Bi–8Zn alloy should have played more or less the same role as hard particles in yielding strain incompatibilities during deformation that leads to misorientation accumulations and formation of new LAGBs boundaries and their

further evolution to HAGBs, i.e., promoting CDRX. Furthermore, the deformation structure was already dominated by submicron grains in regions close to the secondary phase particles. The role of the Bi particles during deformation has been postulated to be twofold. First, they limit slip distances within the structure, and the interaction of dislocations with particles leads to rapid accumulation of dislocation debris. Second, they probably act as dislocation sources, so that dislocation nucleation becomes very easy throughout the structure.

From comparison of the microstructural evolution of the Al–8Zn and Al–6Bi–8Zn alloy, it is apparent that new LAGBs can be rapidly induced around coarse soft particles at relatively low strains and that the initial scale of the grain subdivision process is refined. With increasing strain, these LAGBs evolved into HAGBs, thus increasing the density of HAGB grains. Bi particles were responsible for the much more rapid building up in the fraction of new HAGBs seen at medium to high strains of the Al–6Bi–8Zn alloy, which is similar to the case of large hard intermetallic particles around which complex dislocation structures and particle deformation zone are formed due to the incompatibility between the particles and ductile matrix. However, for composites containing hard particles, there is a shortcoming that during ECAP, they are prone to crack due to particle breaking-up and void formation around particles, which limits the deformation processing at room temperature (RT) [18]. Thereafter, soft particles can be more favourable for accelerating grain refinement during the SPD process.

3.2 Hardness evolution during ECAP

Figure 5 shows the hardness evolution of the Al–8Zn and Al–6Bi–8Zn alloys with increasing ECAP passes.

In the as-cast state (prior to ECAP processing), the hardness of the Al–6Bi–8Zn alloy was slightly lower than that of the Al–8Zn alloy due to the lower hardness of the soft Bi particles. During ECAP deformation, the hardness of the Al–8Zn alloy saturated much more rapidly than the Al–6Bi–8Zn alloy and reached a plateau at HV ~67 at a strain of ~3 (3P), which was consistent with the grain size development in the 3 passes and 5 passes samples. In contrast, after the first pass, hardness of the Al–6Bi–8Zn alloy increased faster than the Al–8Zn alloy, which means that Bi particles contribute to the generation of dislocations (LAGB and/or HAGBs). During the second to the fifth pass, the hardness of the Al–6Bi–8Zn alloy continued to gradually strain harden up to an effective strain of ~5, resulting in the hardness of HV ~73, which was higher than that of the Al–8Zn alloy.

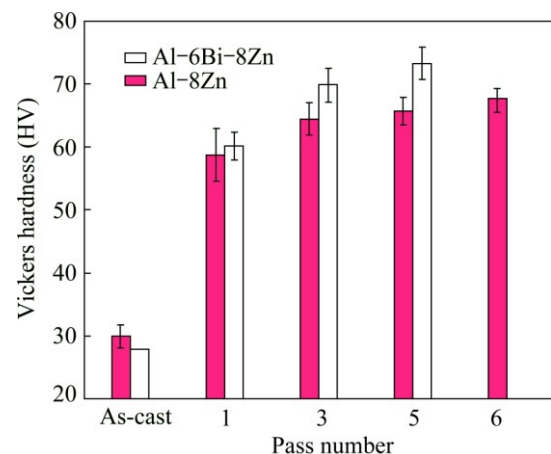


Fig. 5 Comparison of hardness development for Al–8Zn and Al–6Bi–8Zn alloys as function of ECAP passes

4 Conclusions

1) Al–8Zn and Al–6Bi–8Zn alloys were processed at room temperature by ECAP. After 5 passes, ultrafine grained microstructures formed in both alloys. Ultrafine grains down to ~0.5 μm were developed in the Al–6Bi–8Zn alloy which is almost half of the grain size of the Al–8Zn alloy.

2) During ECAP, the original as-cast coarse grains were significantly refined through accelerated CDRX stimulated by the presence of soft Bi particles.

3) After 5 passes of ECAP, a hardness of HV ~73 was achieved in the Al–6Bi–8Zn alloy, which was higher than that of the Al–8Zn alloy due to the finer grain size.

References

- [1] RATKE L, DIEFENBACH S. Liquid immiscible alloys [J]. *Materials Science and Engineering R*, 1995, 15: 263–347.
- [2] GRUBER-PRETZLER M, MAYER F, WU M, MOISEEV J, TONN B, LUDWIG A. Continuous casting of hypermonotectic AlBiZn alloys: Experimental investigations and numerical simulation [C]//Continuous casting. KGaA: Wiley-VCH Verlag GmbH & Co, 2006: 194–201.
- [3] WANG Tong-min, CAO Fei, CHEN Zong-ning, KANG Hui-jun, ZHU Jing, FU Ya-nan, XIAO Ti-qiao, LI Ting-ju. Three dimensional microstructures and wear resistance of Al–Bi immiscible alloys with different grain refiners [J]. *Science China Technological Sciences*, 2015, 58: 870–875.
- [4] SCHAFFER P L, MATHIESEN R H, ARNBERG L. L2 droplet interaction with α -Al during solidification of hypermonotectic Al–8wt.% Bi alloys [J]. *Acta Materialia*, 2009, 57: 2887–2895.
- [5] SILVA A P, SPINELLI J E, MANGELINCK-NOËL N, GARCIA A. Microstructural development during transient directional solidification of hypermonotectic Al–Bi alloys [J]. *Materials & Design*, 2010, 31: 4584–4591.
- [6] SILVA A P, SPINELLI J E, GARCIA A. Microstructural evolution during upward and downward transient directional solidification of hypomonotectic and monotectic Al–Bi alloys [J]. *Journal of Alloys and Compounds*, 2009, 480: 485–493.
- [7] SILVA A P, SPINELLI J E, GARCIA A. Thermal parameters and

- microstructure during transient directional solidification of a monotectic Al–Bi alloy [J]. *Journal of Alloys and Compounds*, 2009, 475: 347–351.
- [8] VALIEV R Z, LANGDON T G. Principles of equal-channel angular pressing as a processing tool for grain refinement [J]. *Progress in Materials Science*, 2006, 51: 881–981.
- [9] ZHA Min, LI Yan-jun, MATHIESEN R H, ROVEN H J. Dispersion of soft Bi particles and grain refinement of matrix in an Al–Bi alloy by equal channel angular pressing [J]. *Journal of Alloys and Compounds*, 2014, 605: 131–136.
- [10] KUHLMANN-WILSDORF D. Overview No. 131 “Regular” deformation bands (DBs) and the LEDS hypothesis [J]. *Acta Materialia*, 1999, 47: 1697–1712.
- [11] BAY B, HANSEN N, HUGHES D A, KUHLMANN-WILSDORF D. Overview No. 96 evolution of f.c.c. deformation structures in polycrystalline [J]. *Acta Metallurgica et Materialia*, 1992, 40: 205–219.
- [12] ZHA Min, LI Yan-jun, MATHIESEN R H, BJØRGE R, ROVEN H J. Microstructure evolution and mechanical behavior of a binary Al–7Mg alloy processed by equal-channel angular pressing [J]. *Acta Materialia*, 2015, 84: 42–54.
- [13] CASTAN C, MONTHEILLET F, PERLADE A. Dynamic recrystallization mechanisms of an Fe–8% Al low density steel under hot rolling conditions [J]. *Scripta Materialia*, 2013, 68: 360–364.
- [14] HUANG Yan, ROBSON J D, PRANGNELL P B. The formation of nanograin structures and accelerated room-temperature theta precipitation in a severely deformed Al–4wt.% Cu alloy [J]. *Acta Materialia*, 2010, 58: 1643–1657.
- [15] JAZAERI H, HUMPHREYS F J. The transition from discontinuous to continuous recrystallization in some aluminium alloys: I—The deformed state [J]. *Acta Materialia*, 2004, 52: 3239–3250.
- [16] APPS P J, BERTA M, PRANGNELL P B. The effect of dispersoids on the grain refinement mechanisms during deformation of aluminium alloys to ultra-high strains [J]. *Acta Materialia*, 2005, 53: 499–511.
- [17] APPS P J, BOWEN J R, PRANGNELL P B. The effect of coarse second-phase particles on the rate of grain refinement during severe deformation processing [J]. *Acta Materialia*, 2003, 51: 2811–2822.
- [18] MUÑOZ-MORRIS M A, GUTIERREZ-URRUTIA I, MORRIS D G. Effect of equal channel angular pressing on strength and ductility of Al–TiAl composites [J]. *Materials Science and Engineering A*, 2005, 396: 3–10.

铋粒子相在大变形过程中对晶粒细化的影响

贾海龙, K. MARTHINSEN, 李彦军

Department of Materials Science and Engineering,
Norwegian University of Science and Technology, Trondheim 7491, Norway

摘 要: 通过背散射电子衍射(EBSD)研究 Al–8Zn 和 Al–6Bi–8Zn 两种合金经 5 道次室温等径角挤压(ECAP)过程中的组织演变和晶粒细化行为。经过 5 道次等径角挤压, 两种合金都形成了超细晶粒。然而, Al–6Bi–8Zn 合金的晶粒明显小于 Al–8Zn 合金, 这说明在等径角挤压过程中铋粒子对晶粒细化有明显的作用。通过测定等径角挤压后两种合金的硬度发现, 经 5 道次等径角挤压之后, Al–6Bi–8Zn 合金的硬度高于 Al–8Zn 合金。此外, 讨论了铋粒子在等径角挤压过程中对变形行为及最终合金强度的影响。

关键词: 铝合金; 等径角挤压; 铋粒子; 晶粒细化; 硬度

(Edited by Xiang-qun LI)